

Reentrant superconductivity in a hybrid heterostructure with a high transparency barrier

E. E. Zubov

G. V. Kurdyumov Institute for Metal Physics, National Academy of Science of Ukraine, Kyiv 03142, Ukraine

Department for Research, Joint Research Laboratory for Dynamics of Electronic Processes in Hybrid Structures, Vasyl' Stus Donetsk National University, Vinnytsia 21021, Ukraine

E-mail: eezubov@ukr.net

Received June 22, 2021, published online October 25, 2021

Within the framework of the self-consistent effective field approximation of the time-dependent perturbation theory, an influence of the electron tunneling on the spontaneously induced order parameters in a normal metal–superconductor hybrid structure is considered. For a normal-metal model, which does not take into account electron–electron scattering, as well as electron–phonon coupling, a critical barrier transparency, corresponding to the disappearance of superconductivity in the ground state, was obtained. The presence of incoherent excitations leads to a complex relationship between the effects of ordering, thermal fluctuations, and tunneling. Near the critical barrier transparency, this can stabilize a superconducting state in the certain temperature intervals. As a result, a reentrant superconductivity phenomenon was observed. The studied spectral properties of the hybrid structure reflect the existence of both coherent and incoherent elementary excitations.

Keywords: superconductivity, critical temperature, hybrid structure, tunnel barrier, proximity effect, coherence effect.

1. Introduction

Despite a long history of the transport properties studies of the normal metal–superconductor hybrid structures, the problem of a rigorous quantum-mechanical analysis of the proximity effect in such systems has not yet lost its relevance. This is especially evident in recent years in connection with the search and realization of Majorana fermions based on the proximity effect in the system of a superconductor with an s -symmetry gap and topological insulator with conducting surface states [1]. This type of fermions is protected from decoherence and is of promising importance in the formation of qubit states for quantum computers. The problem of inhomogeneous superconductivity as a quantum effect is rather complicated from the point of view of subsequent accounting for the correlation effects and the influence of barriers in heterostructures. To date, a wide range of theoretical methods for analyzing the observed experimental electron-tunneling data have been developed. They are based on the well-known equations of Gor'kov [2], Bogolyubov, de Gennes [3], McMillan [4] and their semi-classical approximations [5, 6]. It should be noted that, as a rule, in the study of critical temperatures, spectral and transport properties of hybrid structures consisting of a superconductor and normal magnetic or nonmagnetic metals,

a linear integral relationship is used for the coordinate dependence of the gap function using a nonlocal kernel [7–9]. However, in the case of sufficiently transparent barriers, when a perturbation in the form of a tunnel Hamiltonian is significant, it is no longer possible to consider a linear approximation, since the contribution of electron correlations and scattering may turn out to be significant. In particular, the emergence of reentrant superconductivity, found in Nb/Cu_{1-x}Ni_x bilayers [10], can be associated not only with the ferromagnetism of a normal metal but also with the effect of electron tunneling through a transparent barrier.

It is worth noting that reentrant superconductivity in a hybrid structure ferromagnet–superconductor (F/S) has a complicated origin [8]. In particular, in series of experiments [11, 12], it was observed a nonmonotonic dependence of the critical temperature T_C on the thickness d_F of the ferromagnet in Gd/Nb samples. The authors assumed that such dependence $T_C(d_F)$ was due to the oscillatory behavior of the condensate function in the ferromagnet. Measurements of V/FeV bilayers [13] showed that the interface transparency plays a crucial role in nonmonotonic or monotonic dependence $T_C(d_F)$. In the work [14], the phenomenon of periodical reentrant superconductivity in F/S systems was explained as a combination of the BCS pairing and the Fulde–Ferrel–Larkin–Ovchinnikov (FFLO)

mechanism in S and F layers, respectively. The experimental measurement methods of both reentrant and nonequilibrium superconductivity are presented in the papers [15–19].

Earlier, we presented an effective field approximation in the framework of a diagrammatic approach of the perturbation theory for solving a wide range of problems in condensed matter physics [20]. In particular, in the zeroth approximation over an inverse effective radius of electron interactions, it is possible to build a quantum nonlinear theory of the proximity effect in a hybrid structure normal metal–superconductor with a tunnel barrier [21], in which there are no the phenomenological parameters. Since electron-electron scattering is not taken into account in the Hamiltonian, this model corresponds to the ballistic limit, when a mean free path is substantially greater than the film thickness. Such parameters of superconductivity as the coherence length or the penetration depth of superconducting correlations into a normal metal are derivatives of the theory and can be expressed in terms of the introduced microscopic parameters of the Hamiltonian and temperature. Below the numerical calculations will be done for Sn, Pb, and Al with electron-phonon coupling constants $\lambda = 0.245, 0.39,$ and $0.175,$ respectively. Their Debye frequencies ω_D are 195, 96, and 423 K, respectively [22, 23]. It is supposed that Fermi energy $\mu = 6$ eV.

The structure of the paper is as follows. In the second section, the tunneling Hamiltonian of the hybrid structure normal metal–superconductor (N metal–SC) with the main microscopic parameters of interactions is presented. The presence of ferromagnetism in the normal metal is also assumed. The main goal of this section is to study the inverse proximity effect with reentrant superconductivity for high transparency barriers. The contributions to Green’s functions taking into account the adiabatic switching on the interactions caused by the tunneling Hamiltonian, as well as the appearance of imaginary parts, responsible for electron scattering, to a magnitude and a phase of the spontaneous order parameter have been calculated. The results of numerical calculations of phase diagrams for the inverse proximity effect and spectral characteristics of SC are presented. In the third section, an influence of the tunnel SC electrons on the order parameter, an excitation spectrum, and the spectral density of the N metal part in the hybrid structure is studied. In the fourth section, the main conclusions of the article are formulated.

2. Inverse proximity effect and reentrant superconductivity in a normal metal–superconductor hybrid structure

In a general case, the Hamiltonian for the considered hybrid structure can be written as the sum of Hamiltonians \hat{H}_N, \hat{H}_S for N metal and SC, respectively, as well as the tunnel contribution \hat{H}_T :

$$\hat{H} = \hat{H}_N + \hat{H}_S + \hat{H}_T, \quad (1)$$

where for a N metal in the site representation for the second quantized electron creation (annihilation) operators $c_{\sigma i}^+ (c_{\sigma i})$ with a spin σ

$$\hat{H}_N = \sum_{i,j,\sigma} t_{ij} c_{\sigma i}^+ c_{\sigma j} - \sum_{i\sigma} \mu_{\sigma} c_{\sigma i}^+ c_{\sigma i}. \quad (2)$$

Here, t_{ij} is the hopping integral, which determines the electron band energy, $\mu_{\sigma} = \mu_1 + \sigma J_0,$ μ_1 is the chemical potential for the N metal, J_0 is the parameter of electron exchange interactions, and $J_0 > 0$ for the ferromagnet. Also, $\sigma = \pm 1$ for a saturated state and $\sigma = \pm 2 \langle \sigma_z \rangle$ for the magnet with a mean spin $\langle \sigma_z \rangle.$

For the superconducting part of this structure, we write the Hamiltonian in a mean field approximation

$$\begin{aligned} \hat{H}_S = \sum_{i,j,\sigma} t_{2ij} a_{\sigma i}^+ a_{\sigma j} - \sum_{ij\sigma} (\Delta_{ij\sigma} a_{i\sigma}^+ a_{j-\sigma}^+ + \Delta_{ij\sigma}^* a_{j-\sigma} a_{i\sigma}) \\ - \mu_2 \sum_{i\sigma} a_{\sigma i}^+ a_{\sigma i}, \end{aligned} \quad (3)$$

where μ_2, t_{2ij} and $\Delta_{ij\sigma}$ are the SC chemical potential, an electron band energy and the gap function, respectively. The Fourier transform for the gap function $\Delta_{ij\sigma},$ taking into account that the annihilation operator

$$a_{i\sigma} = \frac{1}{\sqrt{N}} \sum_{\mathbf{k}} e^{i\mathbf{k}R_i} a_{\mathbf{k}\sigma},$$

where N is the number of the SC sites, has a standard BCS self-consistent equation

$$\Delta_{\mathbf{k}\sigma} = \sum_{\mathbf{q}} V_{\mathbf{k}-\mathbf{q}}^{\text{el-ph}} \langle a_{-\mathbf{q}-\sigma} a_{\mathbf{q}\sigma} \rangle. \quad (4)$$

Here $V_{\mathbf{k}}^{\text{el-ph}}$ and $\langle a_{-\mathbf{q}-\sigma} a_{\mathbf{q}\sigma} \rangle$ are the Fourier transform of the electron-phonon coupling parameter and the order parameter as an abnormal correlator, respectively. In [20], we presented a method based on averaging over the unperturbed site Hamiltonians

$$\hat{H}_{0N} = - \sum_{i\sigma} \mu_{\sigma} c_{\sigma i}^+ c_{\sigma i}, \quad (5)$$

$$\hat{H}_{0S} = - \mu_2 \sum_{i\sigma} a_{\sigma i}^+ a_{\sigma i} \quad (6)$$

for N metal and SC, respectively. In this case, the calculation of correlators in a site representation for series of the time perturbation theory with perturbations $V_N = \hat{H}_N - \hat{H}_{0N}, V_S = \hat{H}_S - \hat{H}_{0S},$ and \hat{H}_T for ferromagnetic (FM) normal metal, SC, and the tunnel Hamiltonian $\hat{H}_T,$ respectively, do not present any difficulties. Also, \hat{H}_T is written in a site representation as

$$\hat{H}_T = \sum_{il\sigma} \{ T_{il} c_{i\sigma}^+ a_{l\sigma} + T_{il}^* a_{l\sigma}^+ c_{i\sigma} \}, \quad (7)$$

where T_{il} is an interstitial tunnel matrix element.

To find the abnormal correlator $\langle a_{-\mathbf{q}-\sigma} a_{\mathbf{q}\sigma} \rangle,$ which determines a spontaneous order parameter in an SC, it is necessary to introduce the total causal Green’s functions:

$$\begin{aligned}
 Z_{-q-\sigma}^{--}(\tau) &= -\langle T a_{-q-\sigma}(\tau) a_{q\sigma}(0) \rangle, \\
 Z_{q\sigma}^{+-}(\tau) &= -\langle T a_{q\sigma}^+(\tau) a_{q\sigma}(0) \rangle, \\
 Y_{-pq-\sigma}^{--}(\tau) &= -\langle T c_{-p-\sigma}(\tau) a_{q\sigma}(0) \rangle, \\
 Y_{pq\sigma}^{+-}(\tau) &= -\langle T c_{p\sigma}^+(\tau) a_{q\sigma}(0) \rangle. \quad (8)
 \end{aligned}$$

The spontaneous gap function of a SC is determined by the formula [20]

$$\langle a_{-q-\sigma} a_{q\sigma} \rangle = -\beta \sum_i \text{Res} \left[Z_{-q-\sigma}^{--}(\omega) (f(\omega) - 1) \right]_i, \quad (9)$$

where symbol $\text{Res} [\dots]$ denotes the residues of the Green's function $Z_{-q-\sigma}^{--}(\omega)$ with a factor $f(\omega) - 1$. Here, $f(\omega) = 1 / (\exp(\omega/T) + 1)$ is the Fermi distribution function. The analytic continuation $i\omega_n \rightarrow \omega + i\delta$ for $Z_{q\sigma}^{+-}(i\omega_n) = -Z_{q\sigma}^{+-}(-i\omega_n)$ allows us to find the spectrum and the spectral density of electron-hole excitations of the Cooper pairs condensate:

$$R_{\sigma}(\mathbf{q}, \omega) = -2\beta \text{Im} Z_{q\sigma}^{+-}(\omega + i\delta), \quad (10)$$

the degree of coherence of which is determined by the imaginary part of its poles. Obviously, the scattering of electrons depends only on the tunnel barrier.

Using the scattering matrix, one can form infinite series of expansions for the Green's functions. In particular, in the zeroth approximation over the inverse effective interaction radius, when loop diagrams are not taken into account, it is easy to summarize diagrams of the same type graphically within the framework of the well-known Dyson equation (see details in Appendix). Then we obtain

$$\begin{aligned}
 & Z_{-q-\sigma}^{--}(i\omega_n) \\
 &= \frac{\Delta_{q\sigma} / \beta}{\left[i\omega_n - \xi_{\mathbf{q}} - \tilde{\varphi}_{1-\sigma}(i\omega_n) \right] \left[i\omega_n + \xi_{\mathbf{q}} - \tilde{\varphi}_{2\sigma}(i\omega_n) \right] - |\Delta_{q\sigma}|^2}, \\
 & Z_{q\sigma}^{+-}(i\omega_n) \\
 &= \frac{\left[i\omega_n - \xi_{\mathbf{q}} - \tilde{\varphi}_{1-\sigma}(i\omega_n) \right] / \beta}{\left[i\omega_n - \xi_{\mathbf{q}} - \tilde{\varphi}_{1-\sigma}(i\omega_n) \right] \left[i\omega_n + \xi_{\mathbf{q}} - \tilde{\varphi}_{2\sigma}(i\omega_n) \right] - |\Delta_{q\sigma}|^2}, \quad (11)
 \end{aligned}$$

where $\xi_{\mathbf{q}} = \varepsilon_{2\mathbf{q}} - \mu_2$ is the band energy of electrons relatively the Fermi level of the SC. It is easy to see from expressions (11) for the Green's functions that the excitation spectrum of a superconductor in a hybrid structure is incoherent, since $\tilde{\varphi}_{1-\sigma}(\omega)$ and $\tilde{\varphi}_{2\sigma}(\omega)$ contain the finite imaginary parts (see below), determined by the tunnel matrix element.

Next, we consider the simplest case $|T_{pq}|^2 = |B|^2$, when the tunnel matrix element does not depend on the wave vectors. The frequency ω is supposed to be complex and $|\omega/\mu_1| \ll 1$. Taking into account that the electron density of

states $\rho_N(\varepsilon) = C_N \sqrt{\varepsilon}$, where the constant C_N is proportional to the volume V_N of the N metal, we get

$$\begin{aligned}
 \tilde{\varphi}_{1-\sigma}(\omega) &= \varphi_0(\omega, \Gamma_N) = -\Gamma_N \left(2 + \ln \left(\frac{\omega}{4\mu_1} \right) \right), \\
 \tilde{\varphi}_{2\sigma}(\omega) &= \Gamma_N \left(2 + \ln \left(\frac{-\omega}{4\mu_1} \right) \right), \quad (12)
 \end{aligned}$$

where the value $\Gamma_N = |B|^2 \rho_N(\mu_1)$ determines the barrier transparency for electrons of the N metal. It is also clear that the contribution from magnetism under the sign of the logarithm is infinitesimal of a higher order than $|\omega/\mu_1|$. Therefore, an influence of the magnetic ordering of the N metal on SC can be neglected and the spin indices in Eq. (12) may be disregarded. Obviously, it is true for an equilibrium situation, and in a nonequilibrium case (for example, under the injection of spin-polarized electrons into a superconductor) the effect will be very pronounced [8].

Since the branch cut of complex functions (12) lies on the negative frequency axis ω , it is necessary to take into account the following relation:

$$\ln(\omega) - \ln(-\omega) = i\pi \text{sign}(\arg \omega). \quad (13)$$

One can write an equation for pole singularities of the Green's functions (11) and find the gap in SC:

$$\begin{aligned}
 & \omega^2 - \omega [\tilde{\varphi}_1(\omega) + \tilde{\varphi}_2(\omega)] + \xi_{\mathbf{q}} [\tilde{\varphi}_2(\omega) - \tilde{\varphi}_1(\omega)] \\
 & + \tilde{\varphi}_1(\omega) \tilde{\varphi}_2(\omega) - \xi_{\mathbf{q}}^2 - |\Delta_{q\sigma}|^2 = 0, \quad (14)
 \end{aligned}$$

where $\tilde{\varphi}_{1-\sigma}(\omega) = \tilde{\varphi}_1(\omega)$ and $\tilde{\varphi}_{2\sigma}(\omega) = \tilde{\varphi}_2(\omega)$ in accordance with aforesaid. Formally, this equation can be considered as quadratic with respect to the complex frequency ω . It allows to write an implicit solution in the form

$$\begin{aligned}
 & \omega_{q\sigma}^{\pm} = -\frac{1}{2} i\pi \Gamma_N \text{sign}(\arg \omega_{q\sigma}^{\pm}) \\
 & \pm \sqrt{\left(\xi_{\mathbf{q}} - \Gamma_N \left(2 + \ln \left[\frac{\omega_{q\sigma}^{\pm}}{4\mu_1} \right] \right) + \frac{1}{2} i\pi \Gamma_N \text{sign}(\arg \omega_{q\sigma}^{\pm}) \right)^2 + |\Delta_{q\sigma}|^2}. \quad (15)
 \end{aligned}$$

Unfortunately, Eq. (15) is transcendental relative to the unknown $\omega_{q\sigma}^{\pm}$. However, it is easy to obtain the solutions for both electron and hole excitations by the iteration procedure. As a start, it is necessary to set $\omega_{q\sigma} = E_{q\sigma} + i\delta$, which corresponds to the analytic continuation of the Green's functions to the complex upper half-plane. The iterative procedure for calculating the roots determines solutions with imaginary parts of opposite signs for each root. This uncertainty for the roots is due to the fact, that the replacement $\omega \rightarrow \omega + i\delta$ at the analytic continuation of Green's functions (11) for each iteration step in Eq. (15) because logarithm gives roots on opposite edges of the branch cut. It is clear that the first step of the iteration determines the sign

of the imaginary part of the pole, and the next step of the opposite sign is associated with violation of the selected condition for interaction adiabatic switching on. It is interesting to note that in [21] only the first iteration step was applied to Eq. (15). As will be shown below, the rigorous self-consistency over frequencies $\omega_{q\sigma}^{\pm}$ drastically changes the order parameters, which points out on a significant contribution $\ln[\omega_{q\sigma}^{\pm}/4\mu_1]$ to the proximity effect realization in the N metal–SC structure.

Figure 1 shows real and imaginary parts of the poles as functions of the electron energy ξ_q relative to the Fermi energy level at a gap value $\Delta = 6$ K, the barrier transparency $\Gamma_N = 3.49$ K and $\mu_1 = 6$ eV (solid lines). The BCS spectrum (dashed line) is shown for the comparison. It follows from Fig. 1 that the calculated solid lines are shifted to the left relatively the BCS spectrum. It follows from Eq. (15) that the energy for “above condensate” particles increases by tunnel contributions proportional to the Γ_N parameter.

To find the solution $\Delta_{q\sigma}$ from Eq. (4) after knowing self-consistent solutions $\omega_{q\sigma}^+ = \omega_{q\sigma}$ and $\omega_{q\sigma}^- = -\omega_{q\sigma}$ for the poles $Z_{-q-\sigma}^-(\omega)$ from Eq. (9), it is necessary to make an obvious replacement $\tilde{\varphi}_1(\omega) = \tilde{\varphi}_1(\omega_{q\sigma}^+)$ and $\tilde{\varphi}_2(\omega) = \tilde{\varphi}_2(\omega_{q\sigma}^+)$ in Eq. (14). Note that Eq. (14) is invariant under the substitution $\omega_{q\sigma}^+ \rightarrow \omega_{q\sigma}^-$ [see Eq. (A.4) in Appendix]. Thus, the abnormal Green’s function takes the simplest form

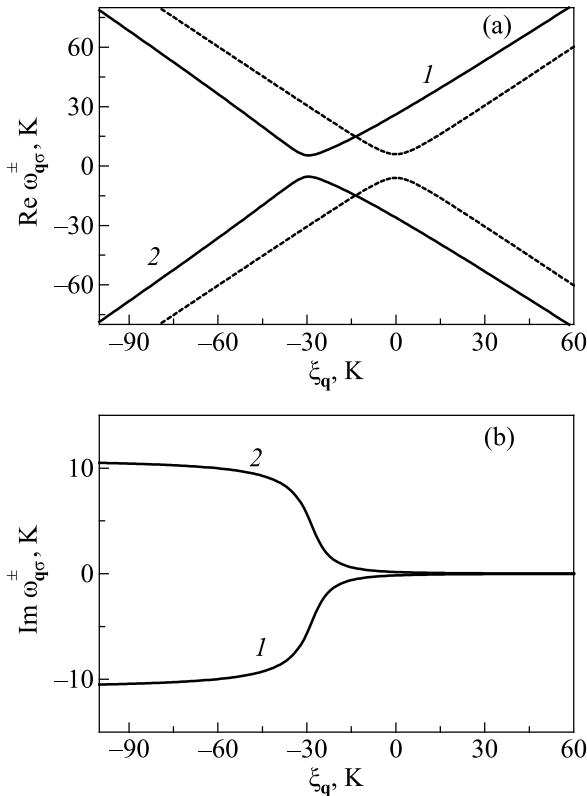


Fig. 1. Real (a) and imaginary (b) parts of the electron and hole spectrum of excitations $\omega_{q\sigma}^+$ and $\omega_{q\sigma}^-$ (solid curves 1 and 2, respectively) for N metal–SC hybrid structure at $\Delta = 6$ K, $\Gamma_N = 3.495$ K and $\mu = 6$ eV, as well as the corresponding coherent BCS spectrum (dashed curves).

$$Z_{-q-\sigma}^-(i\omega_n) = \frac{\Delta_{q\sigma} / \beta}{(i\omega_n - \omega_{q\sigma})(i\omega_n + \omega_{q\sigma})}, \quad (16)$$

that gives for the order parameter

$$\langle a_{-q-\sigma} a_{q\sigma} \rangle = \frac{\Delta_{q\sigma}}{2\omega_{q\sigma}} \tanh\left(\frac{\omega_{q\sigma}}{2T}\right), \quad (17)$$

and the gap function is a complex value for $\Gamma_N \neq 0$, and for $\Gamma_N = 0$ it coincides with the result of the BCS theory. Then, according to Eq. (4), we obtain a self-consistent equation for the complex gap $\Delta_{q\sigma}$:

$$\Delta_{k\sigma} = \sum_q V_{k-q}^{\text{el-ph}} \frac{\Delta_{q\sigma}}{2\omega_{q\sigma}} \tanh\left(\frac{\omega_{q\sigma}}{2T}\right). \quad (18)$$

Assuming the parameter of the electron-phonon interaction $V_{k-q}^{\text{el-ph}} = U$ nonzero near the Fermi level in a narrow energy interval of the order of $\pm \omega_D$, where ω_D is the Debye frequency, let us denote the electron-phonon coupling constant for SC by $\lambda = \rho_F(\mu_2)U$. Here, $\rho_F(\mu_2)$ is the electron density of states at the Fermi surface. Obviously, $\rho_F(\mu_2)$ does not depend on the sample volume. Then one can obtain the integral complex equation for the spontaneous gap:

$$\Delta_{k\sigma} = \lambda \int_{-\omega_D}^{\omega_D} \frac{\Delta_{q\sigma}}{2\omega_{q\sigma}} \tanh\left(\frac{\omega_{q\sigma}}{2T}\right) d\xi_q. \quad (19)$$

In the simple case of the *s*-wave gap with a spatially homogeneous phase, i.e., at $\Delta_{k\sigma} = \Delta = \Delta_S e^{i\varphi}$, where $\Delta_S = |\Delta_{k\sigma}|$ and φ is determined by the rest of the integrand in Eq. (19), which depends on Γ_N . In the approximation $\varphi = \text{const}$ and at $\Gamma_N = 0$ this phase is equal to zero. For a gap under the integral, one can put $\Delta_{q\sigma} = \Delta_S e^{i\varphi}$. Taking the modulus from both sides of Eq. (19) with account for the indicated replacement, we obtain the equation for the gap modulus

$$1 = \lambda \left| \int_{-\omega_D}^{\omega_D} \frac{1}{2\omega_{q\sigma}} \tanh\left(\frac{\omega_{q\sigma}}{2T}\right) d\xi_q \right|. \quad (20)$$

Since the modulus of the right-hand side of Eq. (20) is equal to 1, it can be assumed that the corresponding complex number determines also the gap phase φ , that makes it possible to write

$$\varphi = \arg \left(\lambda \int_{-\omega_D}^{\omega_D} \frac{1}{2\omega_{q\sigma}} \tanh\left(\frac{\omega_{q\sigma}}{2T}\right) d\xi_q \right). \quad (21)$$

Thus, using Eqs. (20), (21), it is possible to calculate an absolute value of the spontaneous gap Δ_S of SC, its phase φ , and the critical temperature T_C of the phase transition, taking into account an influence of the effects of incoherent electrons tunneling in a normal metal.

In Fig. 2, it is shown the dependence of the spontaneous gap Δ_S of the Sn superconductor on the barrier transparency Γ_N at the temperature $T = 0$ K (solid curve), which describes

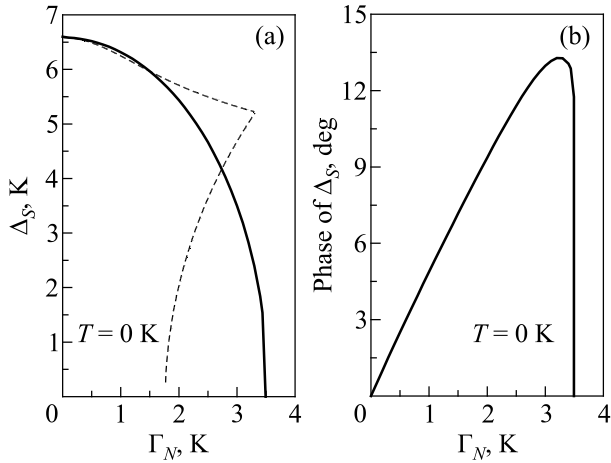


Fig. 2. Dependences of the spontaneous gap Δ_S (a) and its phase (b) of the superconductor Sn on the barrier transparency Γ_N at the temperature $T = 0$ K (solid curve). The dashed curve reflects the same dependence, but without self-consistency over the poles from Eq. (15) [the first iteration step in Eq. (15) [21]].

an inverse proximity effect. The dashed curve was obtained for the poles in Eq. (15) obtained at the first step of the iteration [12].

The critical value of transparency $\Gamma_N = \Gamma_N^{\text{cr}} = 3.495$ K, above which the superconductivity is destroyed, is determined from the equation for T_C at $\tanh(\omega_1(\xi_{\mathbf{q}})/2T) = 1$:

$$F(T, \Gamma_N) = \lambda \int_{-\omega_D}^{\omega_D} \frac{1}{2\omega_1(\xi_{\mathbf{q}})} \tanh\left(\frac{\omega_1(\xi_{\mathbf{q}})}{2T}\right) d\xi_{\mathbf{q}} - 1 = 0, \quad (22)$$

where the frequency $\text{Re}\omega_1(\xi_{\mathbf{q}}) > 0$ and $\omega_1(\xi_{\mathbf{q}})$ is the self-consistent solution of Eq. (15) at $|\Delta_{\mathbf{q}\sigma}| = 0$. Near the high transparency, a role of cooperative phenomena associated with electron-hole scattering by the barrier increases significantly, that is indicated by the phase of the order parameter [see Fig. 2(b)]. On the other hand, the temperature fluctuations partially stabilize the superconducting state, since high-energy electrons from the normal metal are more strongly dissipated. Therefore, with decreasing temperature, an interval of the ordered phase narrows for a highly transparent barrier. In general, the state of itinerant electrons itself is rather complex, that is reflected in the form of a nonmonotonic behavior of the phase transition critical temperature T_C , as well as an appearance of the reentrant superconductivity in certain temperature ranges.

Figure 3 shows that the critical temperature T_C at $\Gamma_N \sim \Gamma_N^{\text{cr}}$ for hybrid structures N metal–Sn and N metal–Pb is the multiple-valued function of Γ_N . Also, T_C strongly fluctuates relative to small changes in Γ_N , when approaches the zero temperature. With further growth of Γ_N , T_C even increases, but in this case superconductivity at low temperatures disappears, and the high-temperature range of the order parameter emergence gradually narrows to zero.

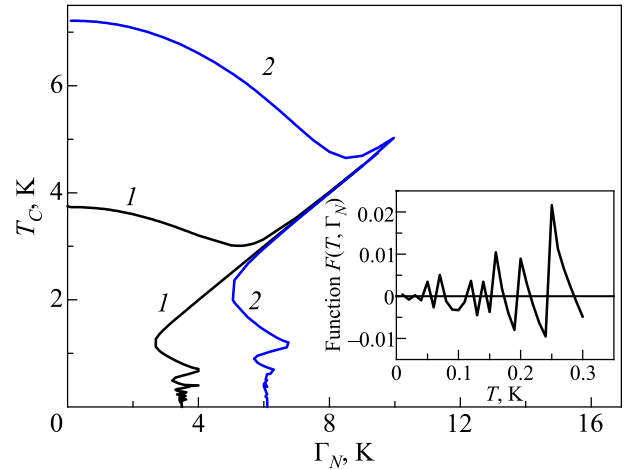


Fig. 3. Phase diagram of the N metal–Sn and N metal–Pb heterostructures (curves 1 and 2, respectively). For Pb, the values $\mu_2 = 9.9$ eV and $\Gamma_N^{\text{cr}} = 6.105$ K are taken. The inset shows the function $F(T, \Gamma_N)$ from Eq. (22) at $\Gamma_N = \Gamma_N^{\text{cr}} = 3.495$ and low T , the zeros of which determine T_C of the superconductor.

Figure 4 demonstrates the temperature dependences of the gap Δ_S of tin in the N metal–Sn hybrid structure for different values of the barrier transparency Γ_N . It can be seen from the figure that at $\Gamma_N \sim \Gamma_N^{\text{cr}}$ the order parameter exists in certain temperature intervals, i.e., in this case an emergence of the reentrant superconductivity is possible. With decreasing temperature and with increasing Γ_N , the range of the superconductivity existence narrows. Also, near one of the critical temperatures, a two-gap state is possible, that may indicate a first-order phase transition. Since the phase of the gap is directly related to the incoherent scattering of tunnel electrons by the barrier, its temperature dependences for different transparencies Γ_N are of interest. Thus, the presented dependences T_C and Δ_S reflect a complex nature of the relationship between incoherent tunneling electron scattering, thermal fluctuations, and coherent Cooper pairing.

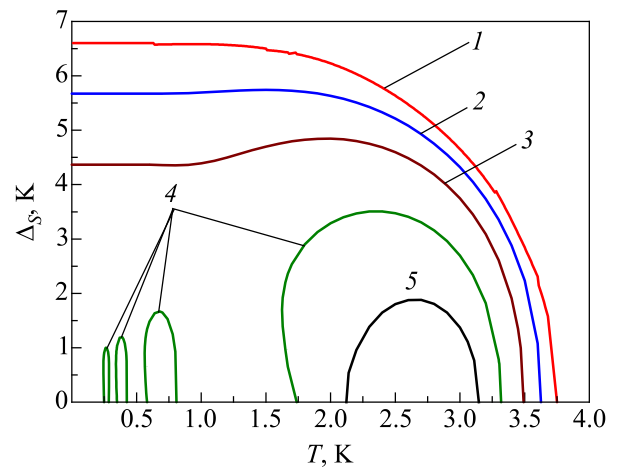


Fig. 4. Temperature dependences of the spontaneous gap Δ_S of the normal metal–tin structure at barrier transparency values $\Gamma_N = 0, 1.8, 2.65, 3.495,$ and 4.25 K (curves 1–5, respectively) with the parameter values from Fig. 3.

3. Proximity effect in ferromagnetic metal

In this section, we will consider an influence of the SC on a ferromagnetic N metal, i.e., the proximity effect associated with the emergence of an induced gap in the specified metal. It has been shown that the magnetic order of an N metal has a negligible effect on an SC. It turns out that the SC significantly affects both transport in a metal due to the proximity effect and its spectral properties. In a similar way as the induced order parameter $\langle c_{-p-\sigma} c_{p\sigma} \rangle$, the spectrum of excitations, and their damping are determined, we can obtain expressions for corresponding electron Green's functions of a metal. Details are presented in the work [20]. Therefore, we can write down expressions for Fourier transforms of the retarded anomalous $Y_{p\sigma}^-(\tau) = -\langle T c_{-p-\sigma}(\tau) c_{p\sigma}(0) \rangle$ and conventional $Y_{p\sigma}^+(\tau) = -\langle T c_{p\sigma}(\tau) c_{p\sigma}^+(\tau) \rangle$ Green's functions of the N metal:

$$Y_{p\sigma}^-(\omega + i\delta) = -\frac{1}{\beta} \frac{\tilde{\beta}(\omega + i\delta)}{\Omega_{p\sigma}(\omega + i\delta)},$$

$$Y_{p\sigma}^+(\omega + i\delta) = \frac{1}{\beta} \frac{\omega + i\delta + \xi_p + J_0\sigma - \tilde{\gamma}(\omega + i\delta)}{\Omega_{p\sigma}(\omega + i\delta)}, \quad (23)$$

where

$$\Omega_{p\sigma}(\omega + i\delta) = \left(\omega + i\delta + \xi_p - J_0\sigma - \tilde{\gamma}(\omega + i\delta) \right) \times \left(\omega + i\delta - \xi_p - J_0\sigma - \tilde{\alpha}(\omega + i\delta) \right) - \left| \tilde{\beta}(\omega + i\delta) \right|^2, \quad (24)$$

$\xi_p = \varepsilon_{1p} - \mu_1$, $\Gamma_S = \rho_S(\mu_2)B^2$ is the barrier transparency for condensate electrons of SC. The expressions for functions $\tilde{\alpha}(\omega)$, $\tilde{\beta}(\omega)$, and $\tilde{\gamma}(\omega)$ are given in Appendix [see Eqs. (A.8)]. The spectrum of excitations is found from pole singularities of the Green's functions, i.e., at the condition $\Omega_{p\sigma}(\omega + i\delta) = 0$ that gives an equation for resonance frequencies ω with account for the analytic continuation $\omega \rightarrow \omega + i\delta$:

$$\omega - J_0\sigma = -\frac{1}{2}i\pi\Gamma_S \frac{\omega}{b(\omega)} \text{sign}(\arg[b(\omega)]) \pm \sqrt{\left(\xi_p - \Gamma_S \left(2 + \ln \left[\frac{b(\omega)}{4\mu_2} \right] \right) - i\pi\Gamma_S \text{sign}(\arg[-b(\omega)]) \right)^2 - \pi^2\Gamma_S^2 \frac{|\Delta|^2}{4b^2(\omega)}}. \quad (25)$$

Here $b(\omega) = \sqrt{\omega^2 - |\Delta|^2}$. The transcendental Eq. (25) has complex roots $\omega_{1\text{op}}$ and $\omega_{2\text{op}}$, which are determined numerically by the iteration procedure.

Figure 5 shows the results for $\omega_{1\text{op}}$ and $\omega_{2\text{op}}$ as functions of energy ξ_p for both paramagnetic and ferromagnetic N metals. It can be seen that for a paramagnet in a certain range of values ξ_p and at frequencies $|\omega| < |\Delta|$, a gap is

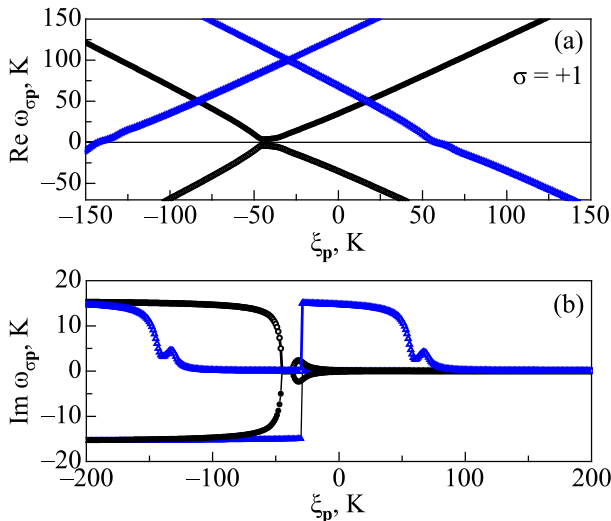


Fig. 5. Real (a) and imaginary (b) parts of excitation electron frequencies $\omega_{1\text{op}}$ (dark circles and triangles) and $\omega_{2\text{op}}$ (open circles and triangles) as functions of the electron energy ξ_p with the barrier transparency $\Gamma_S = 5$ K, the gap $\Delta_S = 6.6$ K and the ferromagnetic exchange $J_0 = 0$ and 100 K (circles and triangles, respectively).

induced in the N metal as a realization of the proximity effect with a nonzero abnormal order parameter $\langle c_{-p-\sigma} c_{p\sigma} \rangle$, which is suppressed by the ferromagnetic exchange. Note that the correlator $\langle c_{-p-\sigma} c_{p\sigma} \rangle$ does not depend on the electron-phonon coupling constant in the N metal and is proportional to the gap Δ , since the N metal is not a superconductor. On the whole, for nonzero Γ_S the spectrum is incoherent while electron excitations with frequencies $|\omega| < |\Delta|$ are coherent [see Eqs. (A.9)–(A.12) in Appendix].

Figure 6 shows the spectrum of coherent electronic excitations $\omega_{1,\text{res}}$ and $\omega_{2,\text{res}}$ [see Eq. (A.10) in Appendix] in a paramagnetic N metal at $\Delta_S = 6.6$ K, $\Gamma_S = 0.5$ and 5 K in the frequency range $|\omega_{i,\text{res}}| < \Delta_S$, as well as the corresponding homogeneous spectral densities of coherent and incoherent excitations from Eq. (25) at $|\omega_{i\text{op}}| > \Delta_S$. In Fig. 6(a), one can see that at $|\omega| < \Delta_S$ in the N metal a forbidden band is also formed, the width of which depends both on the barrier transparency and on the gap of SC. Also, in this case, the induced gap does not depend on the electron-phonon coupling constant in the N metal. The main energy interval of electrons scattered by the barrier is assumed to be near the Fermi level with a width of the order of twice the Debye frequency. The homogeneous spectral density in Fig. 6(b) reflects the coherence of the indicated excitations with an increase in the quasiparticle peak as one approaches boundaries of the forbidden band of the SC and the N metal. It is interesting to note that in the forbidden frequency interval for the N metal, i.e., at $|\omega| < \omega_0(\Gamma_S)$, in contrast to a SC, there are purely complex poles of the Green's function $Y_{p\sigma}^-(\omega + i\delta)$, that point out on a strong electrons scattering.

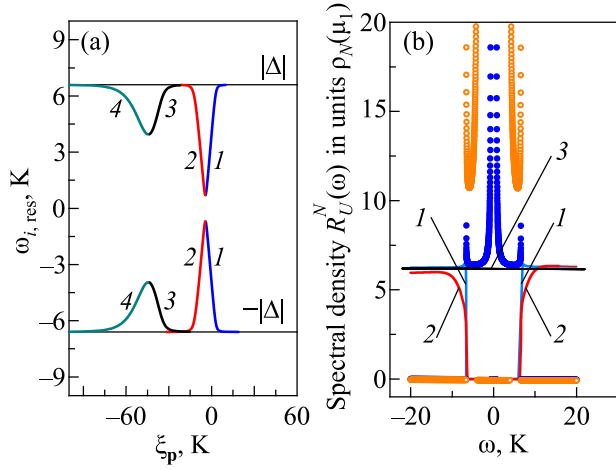


Fig. 6. (a) Spectrum of coherent electron excitations $\omega_{1,res}$ and $\omega_{2,res}$ in a paramagnetic N metal at $|\Delta| = \Delta_S = 6.6$ K and $\Gamma_S = 0.5$ (curves 1 and 2, respectively) and 5 K (curves 3 and 4, respectively) at frequencies $|\omega_{i,sp}| > \Delta_S$; (b) corresponding homogeneous spectral densities of incoherent excitations for $|\omega_{i,sp}| > \Delta_S$ at $\Gamma_S = 0.5$ and 5 K (solid curves 1 and 2, respectively) and those of coherent excitations from (a) at $\Gamma_S = 0.5$ and 5 K (dark and light points, respectively). The straight line 3 corresponds to the spectral density value 2π in units $\rho_N(\mu_1)$ for an N metal with a coherent spectrum.

It can be shown that the corresponding spectral density is identically equal zero, as in the SC.

The problem considered above corresponds to the simplest case, when there is no electron-phonon interaction in the N metal. Here, it is necessary to take into account an

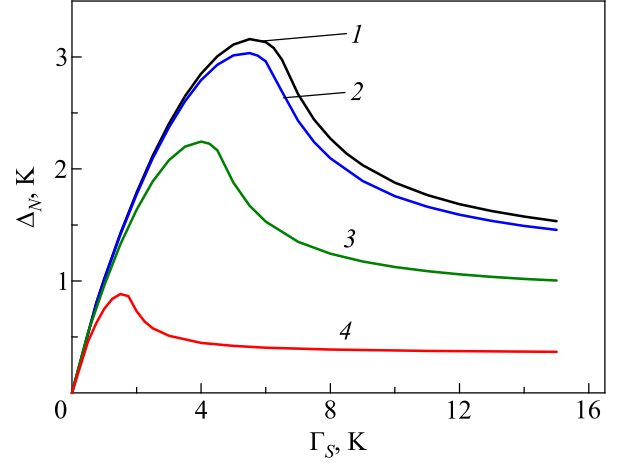


Fig. 7. Gap function Δ_N as a function of the SC transparency Γ_S at the temperature $T = 0$ K for different values of the barrier transparency Γ_N of the N metal: 0.2, 1.0, 2.5, and 3.4 K (curves 1–4, respectively).

effective field in the N metal formed by the order parameter $\langle c_{-p-\sigma} c_{p\sigma} \rangle$ with a corresponding energy gap function

$$\tilde{\Delta}_{\mathbf{k}\sigma} = \sum_{\mathbf{q}} \tilde{v}_{\mathbf{k}-\mathbf{p}}^{\text{el-ph}} \langle c_{-p-\sigma} c_{p\sigma} \rangle, \quad (26)$$

despite $\tilde{\Delta}_{\mathbf{k}\sigma}$ being induced by the effective field of the SC. However, it can be assumed that the induced effective field in the N metal weakly affects the self-consistent SC order parameter, especially for highly transparent barriers. Indeed, the induced homogeneous gap function $\Delta_N = |\tilde{\Delta}_{\mathbf{k}\sigma}|$ reads as

$$\Delta_N = \left| -\frac{1}{2} \tilde{\lambda} i \pi \Gamma_S \Delta \int_{-\tilde{\omega}_D}^{\tilde{\omega}_D} d\xi_p \frac{1}{\omega_{1\text{sp}} - \omega_{2\text{sp}}} \left\{ \frac{[f(\omega_{1\text{sp}}) - 1] \text{sign}(\arg[b(\omega_{1\text{sp}})])}{b(\omega_{1\text{sp}})} - \frac{[f(\omega_{2\text{sp}}) - 1] \text{sign}(\arg[b(\omega_{2\text{sp}})])}{b(\omega_{2\text{sp}})} \right\} \right|, \quad (27)$$

where $\omega_{1\text{sp}}$ and $\omega_{2\text{sp}}$ are the roots of Eq. (25). Figure 7 shows the dependences of a gap Δ_N on the SC transparency Γ_S at temperature $T = 0$ K for various values of Γ_N in Al–Sn hybrid structure. It can be seen that with increasing Γ_S the induced Δ_N increases and then decreases to a value, which then weakly depends on the electron tunneling. Also, with increasing Γ_N , there is a decrease in Δ_N . Note that the value of the spontaneous gap Δ_S in the absence of tunneling is equal to 6.6 K, i.e., significantly exceeds the Δ_N value.

In Fig. 8, the temperature dependences of the induced gap function in Al with $\Gamma_N = 2.65$ K (a) and $\Gamma_N = \Gamma_N^{\text{cr}} = 3.495$ K (b) are shown. It can be seen from Fig. 8(a) that with increasing Γ_S the gap Δ_N increases and then decreases in accordance with Fig. 7. In this case, only for large transparencies Γ_S , nonmonotonic temperature dependence of Δ_N is observed, and for small Γ_S , the induced gap function de-

creases monotonically with increasing T . Figure 8(b) shows the temperature dependences of the reentrant induced superconductivity at the critical value Γ_N , reflecting a rather complex process of proximity effect realization in the hybrid structure.

In conclusion, let us investigate the effect of the FM exchange on the gap in the N metal. As mentioned earlier, the exchange interaction shifts the energy bands up and down, depending on the sign of the spin parameter σ , and decreases the gap (see Fig. 5). Figure 9 shows the gap function Δ_N as a function of the Γ_S transparency of SC at the temperature $T = 0$ for various values of the exchange interaction parameter J_0 and spin indices σ : 0 (curve 1) and 6 K (curves 2 and 3 at $\sigma = 1, -1$, respectively). It can be seen that at $J_0 < \Delta_S$ in the area of the gap maximum for the FM, the exchange suppresses Δ_N , although for high transparencies the decrease

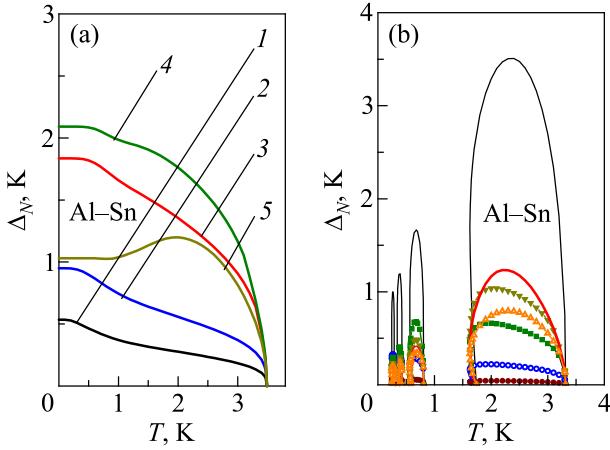


Fig. 8. Temperature dependences of the induced gap function Δ_N in aluminum with $\Gamma_N = 2.65$ (a) and 3.495 (b) K for different barrier transparency Γ_S of tin: (a) $0.5, 1.0, 2.5, 3.5,$ and 10 K (curves 1–5, respectively); (b) 0.1 (dark points), 0.5 (light points), 1.5 (dark squares), 2.5 (dark triangles), 3.5 (solid line), and 10 (light triangles) K. The dotted curve corresponds to the spontaneous reentrant superconductivity at the critical transparency $\Gamma_N = 3.495$ K in Fig. 4.

in Δ_N is not so significant. Also, the gaps for spins $\sigma = 1$ and -1 differ significantly, that is caused by the asymmetric exchange shift of the electron energy bands with corresponding spins. For $J_0 > \Delta_S$, the difficulties arise in calculating Δ_N at low transparencies Γ_S due to oscillations of the integrand in Eq. (27). Therefore, at $J_0 = 10$ K the curve 4 in Fig. 9 ends abruptly at $\Gamma_S = 4$ K.

Conclusions

In this paper, we consider an application of the time perturbation theory to a model in which a self-consistent uniform effective field formed by the electron-phonon

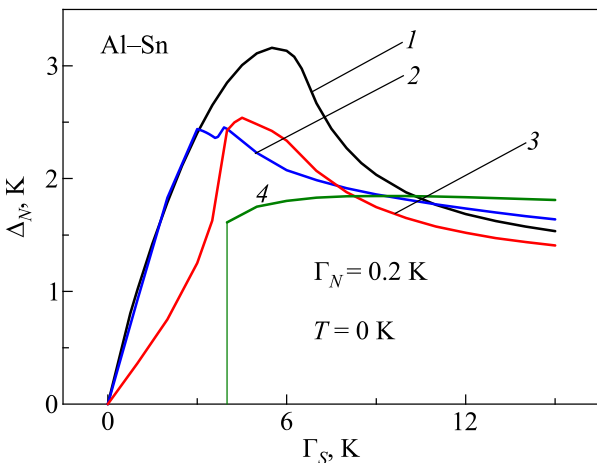


Fig. 9. Induced gap Δ_N as a function of the barrier transparency Γ_S in the ground state for exchange values J_0 equal to 0 (curve 1) and 6 K (curves 2 and 3 at $\sigma = 1, -1$, respectively). Curve 4 corresponds to $J_0 = 10$ K and $\sigma = 1$.

coupling of SC induces an order parameter in the N metal due to electron tunneling processes. The electron-electron scattering is not taken into account that is appropriate for tunnel barriers, the linear sizes of which do not exceed an electron mean free path.

It was found that at the critical transparency Γ_N values of the order of the SC critical temperature T_C , the tunneling electrons of an N metal in the ground state destroy the spontaneous superconductivity. The presence of incoherent excitations leads to a complex relationship between the effects of ordering, thermal fluctuations, and tunneling, which in the vicinity $\Gamma_N \sim \Gamma_N^{\text{cr}}$ can stabilize the superconducting state in certain temperature ranges. Thus, the phenomenon of the reentrant superconductivity is realized. The study of the direct proximity effect showed that a dimensionless order parameter is induced in the N metal in the form of an abnormal correlator, which determines a gap in the spectrum of electron excitations independently of the N metal effective field. This field automatically exists when the electron-phonon interaction in this subsystem is taken into account.

The performed numerical calculations for Al showed that the induced energy gap function is significantly smaller than a gap without the electron-phonon coupling. It was found that the induced gap first increases and then saturates at high transparency Γ_S values. This means that a further increase in the volume of the superconducting part of the hybrid structure has a small effect on the proximity effect. Also, in the range of the gap Δ_N growth as a function of Γ_S , the FM exchange decreases the Δ_N value. The gaps for spin indices $\sigma = 1$ and -1 differ significantly, that is connected with an asymmetric exchange shift of the electron energy bands with corresponding spins. The studied spectral properties of the hybrid structure are in a good agreement with experimental data and reflect the presence of both coherent and incoherent elementary excitations in certain frequency ranges. New detailed experiments dealing with tunneling junctions, where one of the electrodes is a normal metal–superconductor hybrid structure [24], are needed to test our theoretical predictions.

The study was carried out within the Fundamental Research Programme funded by the Ministry of Education and Science of Ukraine (Project No. 0120U102059).

Appendix

Equations for Green's functions and order parameters of a superconductor

In accordance with Hamiltonians (5), (6), the Fourier transforms of the unperturbed Matsubara causal Green's functions for an N metal and a superconductor read as

$$\tilde{G}_{1\sigma}(i\omega_n) = -\left\langle T_{\tau} c_{p\sigma}(\tau) c_{p\sigma}^+(0) \right\rangle_{0, i\omega_n} = \frac{1}{\beta(i\omega_n + \mu_{\sigma})} = -\tilde{G}_{2\sigma}(-i\omega_n),$$

$$G_{1\sigma}(i\omega_n) = -\left\langle T_{\tau} a_{q\sigma}(\tau) a_{q\sigma}^+(0) \right\rangle_{0, i\omega_n} = \frac{1}{\beta(i\omega_n + \mu_2)} = -G_{2\sigma}(-i\omega_n),$$

(A.1)

where the symbol $\langle \dots \rangle_0$ denotes an averaging with Hamiltonians (5) or (6). The imagine frequency $i\omega_n = i\pi(2n + 1)/\beta$ and $1/\beta = T$ is the temperature.

In the zero approximation of a self-consistent field, the above Green's functions are interconnected by means of

$$\begin{aligned} Z_{-q-\sigma}^-(i\omega_n) &= \beta G_1(i\omega_n) \left(\varepsilon_{2-q} Z_{-q-\sigma}^-(i\omega_n) + \Delta_{q\sigma} Z_{q\sigma}^+(i\omega_n) + \sum_{\mathbf{p}} T_{-p-q}^* Y_{-pq-\sigma}^-(i\omega_n) \right), \\ Z_{q\sigma}^+(i\omega_n) &= G_2(i\omega_n) - \beta G_2(i\omega_n) \left(\varepsilon_{2q} Z_{q\sigma}^+(i\omega_n) - \Delta_{q\sigma}^* Z_{-q-\sigma}^-(i\omega_n) + \sum_{\mathbf{p}} T_{pq} Y_{pq\sigma}^+(i\omega_n) \right), \\ Y_{-pq-\sigma}^-(i\omega_n) &= \beta \tilde{G}_{1-\sigma}(i\omega_n) \left(\varepsilon_{1-p} Y_{-pq-\sigma}^-(i\omega_n) + T_{-p-q} Z_{-q-\sigma}^-(i\omega_n) \right), \\ Y_{pq\sigma}^+(i\omega_n) &= \beta \tilde{G}_{2\sigma}(i\omega_n) \left(-\varepsilon_{1p} Y_{pq\sigma}^+(i\omega_n) - T_{pq}^* Z_{q\sigma}^+(i\omega_n) \right), \end{aligned} \quad (\text{A.2})$$

where $\varepsilon_{1p} = \varepsilon_{1-p}$, $\varepsilon_{2q} = \varepsilon_{2-q}$ and T_{pq} are Fourier transforms of the hopping integrals t_{1ij} and t_{2ij} for the N metal, the SC and the tunnel matrix element, respectively. Note that the momentum \mathbf{p} always refers to the N metal, and \mathbf{q} to the SC.

From the system of Eqs. (A.2), in the absence of tunneling, when $T_{ij} = 0$, the trivial solutions $Y_{-pq-\sigma}^-(i\omega_n) = 0$ and $Y_{pq\sigma}^+(i\omega_n) = 0$, and the first two equations coincide with the Gor'kov equations. Taking tunneling into account, the system becomes integral and describes nonlinear proximity effects, since it includes infinite series of contributions to the Green's functions from the tunneling matrix element. Despite the integral character of the system of Eqs. (A.2), it can be easily solved. To do this, from the third and fourth equations we find the unknowns $Y_{-pq-\sigma}^-(i\omega_n)$ and $Y_{pq\sigma}^+(i\omega_n)$ functions and substitute them into the first two equations of the above system, that gives the system of Eqs. (11).

The functions $\tilde{\varphi}_{1-\sigma}(i\omega_n)$ and $\tilde{\varphi}_{2\sigma}(i\omega_n)$, which determine an influence of an N metal on a superconductor, are represented in the form

$$\begin{aligned} \tilde{\varphi}_{1-\sigma}(i\omega_n) &= \sum_{\mathbf{p}} \frac{|T_{pq}|^2}{i\omega_n + (\mu_{-\sigma} - \varepsilon_{1p})}, \\ \tilde{\varphi}_{2\sigma}(i\omega_n) &= \sum_{\mathbf{p}} \frac{|T_{pq}|^2}{i\omega_n - (\mu_{\sigma} - \varepsilon_{1p})}. \end{aligned} \quad (\text{A.3})$$

To determine the spontaneous gap in accordance with Eq. (9), after the analytic continuation $\omega \rightarrow \omega + i\delta$, it is necessary to calculate the functions $\tilde{\varphi}_{1-\sigma}(\omega)$ and $\tilde{\varphi}_{2\sigma}(\omega)$. Obviously, these functions are connected by the relation

$$\tilde{\varphi}_{1-\sigma}(\omega) = -\tilde{\varphi}_{2-\sigma}(-\omega). \quad (\text{A.4})$$

The expression for the spectral density of states $R_{\sigma}(\mathbf{q}, \omega)$ from Eq. (10) reads as

$$R_{\sigma}(\mathbf{q}, \omega) = -2\pi\Gamma_N \frac{\theta(\omega) \left[\omega^2 - \tilde{E}_{\mathbf{q}}^2 \right] - (\omega + \tilde{\xi}_{\mathbf{q}})(\omega - \text{sign}(\omega)\tilde{\xi}_{\mathbf{q}})}{\left[\omega^2 - \tilde{E}_{\mathbf{q}}^2 \right]^2 + \pi^2 \Gamma_N^2 (\omega - \text{sign}(\omega)\tilde{\xi}_{\mathbf{q}})^2}, \quad (\text{A.5})$$

graphical equations in the Fourier space (the details can be found in [20]). In the analytical form, these equations are written as follows:

where $\tilde{E}_{\mathbf{q}}(\omega) = \sqrt{\tilde{\xi}_{\mathbf{q}}^2(\omega) + \Delta_S^2}$, $\tilde{\xi}_{\mathbf{q}}(\omega) = \xi_{\mathbf{q}} + \varphi_0(|\omega|, \Gamma_N)$, $\theta(\omega)$ is the Heaviside step function, and $\varphi_0(\omega, \Gamma_N)$ is the function from Eqs. (12). Let us define the homogeneous spectral density as follows:

$$R_U^S(\omega) = \sum_{\mathbf{q}} R_{\sigma}(\mathbf{q}, \omega) = \rho_S(\mu_2) \int_{-\omega_D}^{\omega_D} d\xi_{\mathbf{q}} R_{\sigma}(\mathbf{q}, \omega), \quad (\text{A.6})$$

where $\rho_S(\mu_2)$ is the bulk electron density of states of a SC metal at the Fermi level.

In Fig. 10, the frequency dependences of a homogeneous spectral density of superconducting Sn at a temperature $T = 0$ K for different Γ_N values and at the critical transparency $\Gamma_N = \Gamma_N^{\text{cr}} = 3.495$ K in the temperature interval from 1.6 to 3.1 K, where the reentrant superconductivity emerges, are shown. It can be seen from Fig. 10(a) that for small Γ_N

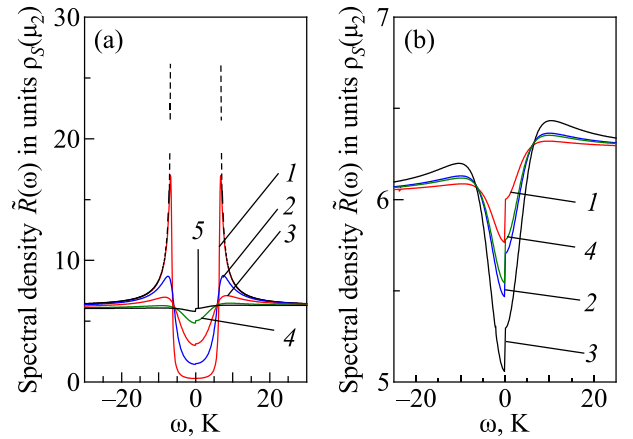


Fig. 10. Frequency dependences of the homogeneous spectral density $\tilde{R}(\omega)$ from (A.6) in units $\rho_S(\mu_2)$ for the superconductor in a hybrid normal metal–Sn structure: (a) at the temperature $T = 0$ K and $\Gamma_N = 0$ ($\Delta_S = 6.6$ K, dashed line), 0.2, 1.0, 2.0, 3.0, and 3.44 K ($\Delta_S = 6.57, 6.32, 5.44, 3.50, 1.54$ K, solid lines 1–5, respectively); (b) at the critical transparency $\Gamma_N = \Gamma_N^{\text{cr}} = 3.495$ K and $T = 1.625, 1.7, 2.4, 3.1$ K ($\Delta_S = 1.7, 2.53, 3.51, 2.34$ K, curves 1–4, respectively).

the $R_V^S(\omega)$ function is close to the conventional $R_G^S(\omega)$ function for a homogeneous superconductor:

$$R_G^S(\omega) = \frac{2\pi\rho_S(\mu_2)|\omega|}{\sqrt{\omega^2 - \Delta_S^2}}. \quad (\text{A.7})$$

With increasing Γ_N , the spectral density $\tilde{R}(\omega)$ approaches a value $2\pi\rho_S(\mu_2)$ that corresponds to an N metal and reflects the inverse proximity effect. In Fig. 10(b), $\tilde{R}(\omega)$ is shown at the critical transparency $\Gamma_N^{\text{cr}} = 3.495$ K, and in the

$$\begin{aligned} \tilde{\alpha}(\omega) &= -\Gamma_S \left\{ 2 + \ln \frac{b(\omega)}{4\mu_2} + \frac{1}{2} i\pi \left[\frac{\omega}{b(\omega)} \text{sign}(\arg[b(\omega)]) + \text{sign}(\arg[-b(\omega)]) \right] \right\}, \\ \tilde{\beta}(\omega) &= -\Delta\Gamma_S \frac{i\pi}{2b(\omega)} \text{sign}(\arg[b(\omega)]), \\ \tilde{\gamma}(\omega) &= \Gamma_S \left\{ 2 + \ln \frac{b(\omega)}{4\mu_2} - \frac{1}{2} i\pi \left[\frac{\omega}{b(\omega)} \text{sign}(\arg[b(\omega)]) - \text{sign}(\arg[-b(\omega)]) \right] \right\}, \end{aligned} \quad (\text{A.8})$$

where $b(\omega) = \sqrt{\omega^2 - |\Delta|^2}$.

Let us prove the coherence of electron excitations in an N metal with frequencies $|\omega| < |\Delta|$. We need it for correct calculations of the corresponding spectral density. Indeed, it is easy to see that at $|\omega| < |\Delta|$ the tunnel functions (A.8) are real. Relatively unknowns $\xi_{\mathbf{p}}$, the equation $\Omega_{\mathbf{p}\sigma}(\omega) = 0$ is quadratic for the integrand pole singularities of the homogeneous spectral density $R_V^N(\omega)$:

$$R_V^N(\omega) = \sum_{\mathbf{p}} \tilde{R}_{\sigma}(\mathbf{p}, \omega) = \rho_N(\mu_1) \int_{-\tilde{\omega}_D}^{\tilde{\omega}_D} d\xi_{\mathbf{p}} \tilde{R}_{\sigma}(\mathbf{p}, \omega), \quad (\text{A.9})$$

where $\tilde{R}_{\sigma}(\mathbf{p}, \omega) = -2\beta \text{Im} Y_{\mathbf{p}\sigma}^{-+}(\omega + i\delta)$ and $\tilde{\omega}_D$ is Debye frequency for the N metal. That is why one can write its solutions $\xi_1(\omega)$ and $\xi_2(\omega)$ in the form

$$\begin{aligned} \xi_{1,2}(\omega) &= \Gamma_S \left(2 + \ln \frac{\tilde{b}(\omega)}{4\mu_2} \right) \\ &\pm \sqrt{\left(\omega + J_0\sigma \right) \left(\omega + J_0\sigma + \Gamma_S \frac{\pi\omega}{\tilde{b}(\omega)} \right) - \frac{1}{4} \pi^2 \Gamma_S^2}, \quad (\text{A.10}) \end{aligned}$$

where $\tilde{b}(\omega) = \sqrt{\Delta_S^2 - \omega^2}$. Obviously, Eq. (A.10) gives poles on the real frequency axis if the radical expression is non-negative. Consider the simplest case $J_0 = 0$. Then at

$$\Gamma_S \leq \frac{2|\omega| \left\{ |\omega| + \Delta_S \right\}}{\pi\sqrt{\Delta_S^2 - \omega^2}} = g(\omega) \quad (\text{A.11})$$

we have the coherent spectrum, if $|\omega| < \Delta_S$ and $|\omega| > g^{-1}(\Gamma_S) = \omega_0(\Gamma_S)$, where $g^{-1}(x)$ is the inverse function from Eq. (A.11). The numerical analysis with analytic continuation $\omega \rightarrow \omega + i\delta$ shows that $\text{sign}(\text{Im}(\xi_1(\omega + i\delta))) = \text{sign}(\omega)$ and $\text{sign}(\text{Im}(\xi_2(\omega + i\delta))) = -\text{sign}(\omega)$. In accordance with the Landau bypass rule, it is easy to find the spectral density

temperature range of the reentrant superconductivity emergence. It can be seen from the figure that in this case, due to a high barrier transparency, an influence of the N metal on the spontaneous order parameter is quite significant. Also, due to the jump at the singular point $\omega = 0$, $\tilde{R}(\omega)$ is asymmetric near the origin. The presented dependences are in good agreement with the known experimental data [25].

The expressions for $\tilde{\alpha}(\omega)$, $\tilde{\beta}(\omega)$, and $\tilde{\gamma}(\omega)$ functions from Eqs. (23), (24) are

of coherent electron excitations in the N metal for frequencies $|\omega| < \Delta_S$:

$$\begin{aligned} R_V^N(\omega) &= \frac{2\pi \text{sign}(\omega) \theta(|\omega| - \omega_0(\Gamma_S)) \theta(\Delta_S - |\omega|) \rho_N(\mu_1)}{\sqrt{\omega(\omega + \Gamma_S \pi\omega / \tilde{b}(\omega)) - \frac{1}{4} \pi^2 \Gamma_S^2}} \\ &\times \left\{ \omega + \Gamma_S \pi\omega / \tilde{b}(\omega) \right\}, \quad (\text{A.12}) \end{aligned}$$

that is shown in Fig. 6(b).

1. A. Yu. Kitaev, *Phys. Usp.* **44**, 131 (2001).
2. L. P. Gor'kov, *Sov. Phys. JETP* **34**, 505 (1958).
3. P. G. de Gennes, *Rev. Mod. Phys.* **36**, 225 (1964).
4. W. L. McMillan, *Phys. Rev.* **175**, 537 (1968).
5. G. Eilenberger, *Z. Phys.* **214**, 195 (1968).
6. K. D. Usadel, *Phys. Rev. Lett.* **25**, 507 (1970).
7. A. Golubov, M. Yu. Kupriyanov, V. Lukichev, and A. Orlikovskiy, *Russ. Microelectron.* **12**, 355 (1983).
8. F. S. Bergeret, A. F. Volkov, and K. B. Efetov, *Rev. Mod. Phys.* **77**, 1321 (2005).
9. A. I. Buzdin, *Rev. Mod. Phys.* **77**, 935 (2005).
10. V. Zdravkov, A. Sidorenko, G. Obermeier, S. Gsell, M. Schreck, C. Muller, S. Horn, R. Tidecks, and L.R. Tagirov, *Phys. Rev. Lett.* **97**, 057004 (2006).
11. J. S. Jiang, D. Davidovic, D. H. Reich, and C. L. Chien, *Phys. Rev. Lett.* **74**, 314 (1995).
12. F. Y. Ogrin, S. L. Lee, A. D. Hillier, A. Mitchell, and T.-H. Shen, *Phys. Rev. B* **62**, 6021 (2000).
13. J. Aarts, J. M. E. Geers, E. Brück, A. A. Golubov, and R. Coehoorn, *Phys. Rev. B* **56**, 2779 (1997).
14. M. G. Khusainov and Yu. N. Proshin, *Phys. Rev. B* **56**, R14283 (1997).
15. Y. Cao, J. M. Park, K. Watanabe, T. Taniguchi, and P. Jarillo-Herrero, *Nature* **595**, 526 (2021).

16. V. Fatemi, S. Wu, Y. Cao, L. Brethau, Q. D. Gibson, K. Watanabe, T. Taniguchi, R. J. Cava, and P. Jarillo-Herrero, *Science* **362**, 926 (2018).
17. S. Uji, H. Shinagawa, T. Terashima, T. Yakabe, Y. Terai, M. Tokumoto, A. Kobayashi, H. Tanaka, and H. Kobayashi, *Nature* **410**, 908 (2001).
18. M. A. Belogolovskii, Yu. F. Revenko, A. Yu. Gerasimenko, V. M. Svistunov, E. Hatta, G. Plitnik, V. E. Shaternik, and E. M. Rudenko, *Fiz. Nizk. Temp.* **28**, 553 (2002) [*Low Temp. Phys.* **28**, 391 (2002)].
19. E. Rudenko, D. Solomakha, I. Korotash, P. Febvre, E. Zhitlukhina, and M. Belogolovskii, *IEEE Trans. Appl. Supercond.* **27**, 1800105 (2017).
20. E. E. Zubov and E. S. Zhitlukhina, *Effective Field Approach to Transition-Metal Oxide Systems: Magnetism, Transport and Spectral Properties*, Vasyli' Stus–DonNU, Vinnytsia, ISBN 978-966-949-157-2 (2019) (see also <http://arxiv.org/abs/1903.05180>).
21. E. E. Zubov, *Nonlinear Proximity Effect in a Hybrid Normal Metal-Superconductor Structure* (2020), *IEEE 10th Intern. Conf. Nanomaterials: Applications & Properties (NAP)*.
22. R. Meservey and B. B. Schwartz, *Equilibrium Properties: Comparison of Experimental Results With Prediction of the BCS Theory*, in *Superconductivity*, vol. I, R. D. Parks (ed.), Marcel Dekker, Inc., New York (1969).
23. G. Gladstone, M. A. Jensen, and J. R. Schrieffer, *Superconductivity in the Transition Metals: Theory and Experiment*, in *Superconductivity*, vol. II, R. D. Parks (ed.), Marcel Dekker, Inc., New York (1969).
24. E. Zhitlukhina, I. Devyatov, O. Egorov, M. Belogolovskii, and P. Seidel, *Nanoscale Res. Lett.* **11**, 58 (2016).
25. S. Guéron, H. Pothier, N. O. Birge, D. Esteve, and M. H. Devoret, *Phys. Rev. Lett.* **77**, 3025 (1996).

Поворотна надпровідність в гібридній гетероструктурі з високою бар'єрною прозорістю

E. E. Zubov

В рамках самоузгодженого наближення ефективного поля часової теорії збурень розглядається вплив тунелювання електронів на спонтанні та індуковані параметри порядку в гібридній структурі нормальний метал–надпровідник. Для моделі без електрон-електронного розсіювання, а також електрон-фононного зв'язку в нормальному металі отримано критичну бар'єрну прозорість, коли надпровідність зникає в основному стані. Наявність некогерентних збуджень призводить до складного взаємозв'язку ефектів упорядкування, теплових флуктуацій та тунелювання. Поблизу критичної бар'єрної прозорості це може стабілізувати надпровідний стан у певних температурних інтервалах. В результаті спостерігається явище поворотної надпровідності. Вивчені спектральні властивості цієї гібридної структури відображають існування як когерентних, так і некогерентних елементарних збуджень.

Ключові слова: надпровідність, критична температура, гібридна структура, тунельний бар'єр, ефект близькості, когерентність.